



Article

Integrated Transcriptome and Metabolomics to Reveal the Mechanism of Adipose Mesenchymal Stem Cells in Treating Liver Fibrosis

Haifeng Liu ^{1,†}, Xinmiao Wang ^{1,†}, Hongchuan Deng ¹, Haocheng Huang ¹, Yifan Liu ¹, Zhijun Zhong ¹, Liuhong Shen ¹, Suizhong Cao ¹, Xiaoping Ma ¹, Ziyao Zhou ¹, Dechun Chen ^{2,*} and Guangneng Peng ^{1,*}

- Department of Veterinary Surgery, College of Veterinary Medicine, Sichuan Agricultural University, Chengdu 611130, China; hfliu@sicau.edu.cn (H.L.); wxm970618@163.com (X.W.); d18784998479@126.com (H.D.); hhc3267074227@163.com (H.H.); shenlh@sicau.edu.cn (L.S.); suizhongcao@126.com (S.C.); mxp886@sina.com.cn (X.M.); 13086613810@165.com (Y.L.); zhongzhijun488@126.com (Z.Z.); zzhou@sicau.edu.cn (Z.Z.)
- ² College of Animal and Veterinary Sciences, Southwest Minzu University, Chengdu 610041, China
- * Correspondence: chendechun@swun.edu.cn (D.C.); pgn.sicau@163.com (G.P.)
- [†] These authors contributed equally to this work.

Abstract: Liver fibrosis (LF) is a late-stage process observed in various chronic liver diseases with bile and retinol metabolism closely associated with it. Adipose-derived mesenchymal stem cells (ADMSCs) have shown significant therapeutic potential in treating LF. In this study, the transplantation of ADMSCs was applied to a CCl₄-induced LF model to investigate its molecular mechanism through a multi-omics joint analysis. The findings reveal that ADMSCs effectively reduced levels of alanine aminotransferase (ALT), aspartate aminotransferase (AST), total bilirubin (TBIL), gammaglutamyltransferase (GGT), Interleukin-6 (IL-6), tumor necrosis factor-alpha (TNF- α), and α -Smooth muscle actin (α -SMA), thereby mitigating liver lesions, preventing liver parenchymal necrosis, and improving liver collagen deposition. Furthermore, 4751 differentially expressed genes (DEGs) and 270 differentially expressed metabolites (DMs) were detected via transcriptome and metabolomics analysis. Conjoint analysis showed that ADMSCs up-regulated the expression of *Cyp7a1*, *Baat*, *Cyp27a1*, *Adh7*, *Slco1a4*, *Aldh1a1*, and *Adh7* genes to promote primary bile acids (TCDCA: Taurochenodeoxycholic acid; GCDCA: Glycochenodeoxycholic acid; GCA: glycocholic acid, TCA: Taurocholic acid) synthesis, secretion and retinol metabolism. This suggests that ADMSCs play a therapeutic role in maintaining bile acid (BA) homeostasis and correcting disturbances in retinol metabolism.

Keywords: adipose-derived mesenchymal stem cells (ADMSCs); liver fibrosis (LF); bile acid (BA); retinol metabolism



Citation: Liu, H.; Wang, X.; Deng, H.; Huang, H.; Liu, Y.; Zhong, Z.; Shen, L.; Cao, S.; Ma, X.; Zhou, Z.; et al. Integrated Transcriptome and Metabolomics to Reveal the Mechanism of Adipose Mesenchymal Stem Cells in Treating Liver Fibrosis. *Int. J. Mol. Sci.* 2023, 24, 16086. https://doi.org/10.3390/ijms242216086

Received: 4 October 2023 Revised: 1 November 2023 Accepted: 6 November 2023 Published: 8 November 2023



Copyright: © 2023 by the authors. Licensee MDPI, Basel, Switzerland. This article is an open access article distributed under the terms and conditions of the Creative Commons Attribution (CC BY) license (https://creativecommons.org/licenses/by/4.0/).

1. Introduction

Any cause of chronic liver disease (hepatitis B and C, alcohol, cholestasis, and non-alcoholic steatohepatitis (NASH)) leads to LF [1]. LF is characterized by the excessive synthesis and deposition of the extracellular matrix (ECM) [2]. Hepatic stellate cells (HSC) are considered major effectors of LF because they are involved in ECM deposition and trigger immune responses by secreting cytokines and chemokines. In the process of HSC activation, on the one hand, HSC can stimulate the secretion of IL-17 in TH17 cells, upregulate the expression of NF-κB and STAT3, and aggravate liver inflammation [3]. On the other hand, the inhibition of the CXCR7-Id1 pathway through the fibroblast growth factor receptor 1 (FGFR 1)-CXCR4 axis inhibits normal liver regeneration and aggravates LF [4]. The activation of HSC is accompanied by a large loss of retinoids, which further aggravates inflammation and fibrosis progression and accelerates the occurrence of liver tumors. Unfortunately, the biological function of retinoid loss in HSC and LF remains unclear. Meanwhile, in liver injury, *Cyp8a1* downregulation inhibits the intrahepatic synthesis of BA

and exacerbates LF [5]. The inactivation of the farnesoid X receptor (FXR) after liver injury leads to an increased BA synthesis rate and fibroblast growth factor 19 (FGF19) expression in the liver, which induces the activation of inflammatory pathways and promotes hepatocyte apoptosis, leading to LF [6,7]. Therefore, inhibiting HSC activation, regulating the level of body and immune response, and correcting metabolic disorders are effective ways to prevent or reduce LF. Unfortunately, there is no generally accepted therapy for the treatment of LF.

ADMSCs have attracted great interest in the field of disease treatment due to their multi-directional differentiation potential and self-renewal ability [8]. The transplantation of ADMSCs has been shown to be effective in the treatment of colitis by inducing a macrophage phenotype shift from M1 to M2 [9]. In addition, extracellular vesicles released by ADMSCs attenuate neuroinflammation associated with Alzheimer's disease via miR-122 [10]. Simultaneously, numerous studies have demonstrated that the transplantation of ADMSCs exhibits therapeutic efficacy in diverse systemic ailments, including kidney, heart, and bone diseases [11,12]. The liver, which is the largest endocrine organ, is susceptible to damage caused by various pathogenic factors, resulting in metabolic disturbances. Studies have shown that transplanted ADMSCs are attracted to damaged liver tissue by various inflammatory factors and chemokines. They promote endogenous hepatocyte regeneration and maintain the normal structure of the liver by secreting cytokines such as the hepatocyte growth factor (HGF) and FGF [13,14]. In the context of liver ischemia-reperfusion injury, ADMSCs have been found to play a role in inhibiting hepatocyte apoptosis. This inhibition is achieved through the up-regulation of the expression of Fas, caspase-3, and caspase-9. Additionally, ADMSCs also demonstrate the ability to suppress hepatocyte autophagy via upregulating superoxide dismutase (SOD) activity [15,16]. Studies have shown that the transplantation of ADMSCs can effectively treat LF by promoting liver differentiation, inhibiting inflammatory response, and suppressing HSC activation [17]. These effects are primarily achieved through the inhibition of LF factors such as nerve growth factor (NGF), transforming growth factor- β 1 (TGF- β 1), α -SMA, hyaluronic acid, and hydroxyproline [17–19]. In clinical practice, the transplantation of ADMSCs has been reported to treat patients with liver cirrhosis [20]. Most studies have demonstrated that the transplantation of ADMSCs can effectively treat liver diseases by regulating the immune system, suppressing inflammation, and reducing LF markers. However, there is currently no report on whether the transplantation of ADMSCs can treat LF by modulating liver metabolic pathways.

Metabolomics is a burgeoning research method that focuses on analyzing endogenous metabolites found in the urine, serum, and tissues [21]. Its aim is to gain a comprehensive understanding of the metabolic pathways within an entire organ or system. Metabolites, which are the products of cellular regulatory processes, serve as valuable indicators of disorders resulting from drugs or diseases. By identifying the metabolic pathways in which differential metabolites are located, metabolomics provides insight into the disrupted metabolic processes associated with disease [22]. The liver, as the largest organ in the body, performs numerous synthetic and secretory functions, making it essential for the body's metabolism [8]. Metabolomics has gained significant popularity in the study of liver diseases due to its effective qualitative and quantitative analysis of metabolites [22,23]. Transcriptomics involves the comprehensive collection of transcriptional information from tissues or organs, enabling the prediction of the potential mechanisms of external substances that stimulate metabolic pathways [24]. Numerous studies have utilized transcriptomics to analyze the gene expression profiles of different liver diseases and predict potential therapeutic targets or toxic effects of drugs on the liver [25,26]. By integrating transcriptomics and metabolomic profiles, researchers can gain a more reliable understanding of metabolic alterations and further investigate the underlying biological processes and toxic mechanisms. Therefore, this experiment aims to explore the mechanism by which ADMSCs affect LF at the transcriptional and metabolic levels.

2. Results

2.1. ADMSCs Alleviate Liver Injury and Fibrosis in Rats

To investigate the effect of ADMSCs on LF models, a rat LF model was established via the intraperitoneal injection of CCl₄, and ADMSCs were used for treatment. Serum biochemistry and Elisa results showed that the expression levels of liver function indicators ALT, AST, TBIL, GGT and inflammatory factors, such as IL-6 and TNF- α , were significantly increased in rats with LF (p < 0.05, Figure 1A–F). However, the expression of the above indicators was significantly downregulated after the transplantation of ADMSCs (p < 0.05). HE and MASSON staining revealed that fibrosis rats exhibited significant liver cell structural damage, intercellular lipid droplets and vacuoles, and collagen fiber deposition compared to the Cont group.

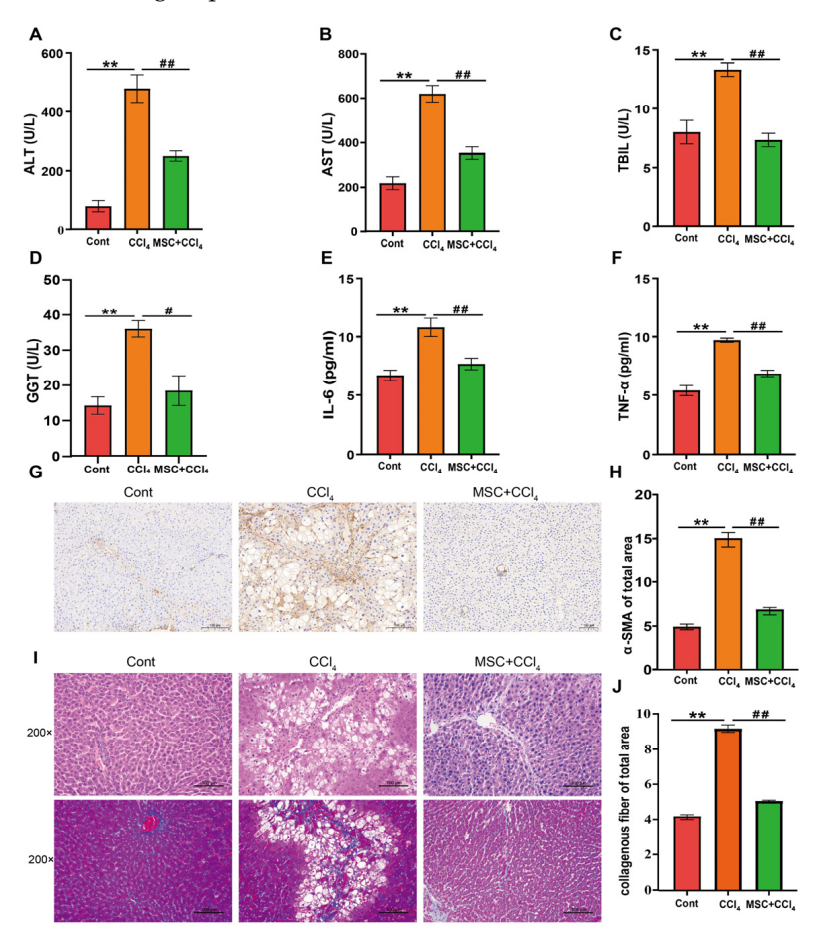


Figure 1. ADMSCs alleviate liver injury and fibrosis in rats. (**A–D**). Biochemical indicator tests of serum (ALT, AST, TBIL, and GGT); (**E,F**). Detection of serum Elisa-related inflammatory indicators (IL-6 and TNF-α); (**G,H**). Immunohistochemistry and the surface ratio of LF marker factor α-SMA (×200 magnification). (**I,J**). H&E staining (upper) (×200 magnification) and MASSOM staining (bottom) (×200 magnification) of the liver in different groups. Each experiment was carried out at least three times, and the data were displayed using the mean \pm SD. Cont, control group; CCl₄, CCl₄, CCl₄ intervention group; MSC, ADMSCs treatment group. **, p < 0.01 vs. Cont group; #, p < 0.05; ##, p < 0.01 vs. MSC group.

However, a significant improvement occurred after ADMSCs treatment (Figure 1I,J). Immunohistochemical methods were used to detect the expression of the LF marker α -SMA. The expression of α -SMA in the liver tissue of the CCl $_4$ group was significantly increased compared to the Cont group. The transplantation of ADMSCs eliminated these protein expression imbalances (Figure 1G,H).

Int. J. Mol. Sci. 2023, 24, 16086 4 of 17

2.2. Changes in Liver Metabolic Profile after Adipose Mesenchymal Stem Cell Transplantation

Three groups of rat liver metabolites were detected using UHPLC-MS/MS, and a total of 1020 metabolites were annotated through a reliable dataBAe. The results of the OPLS-DA analysis indicated significant differences in liver metabolic product patterns between the CCl₄ group and the other two groups, while there were some similarities in liver metabolic products between the Cont and MSC groups (Figure 2A,B).

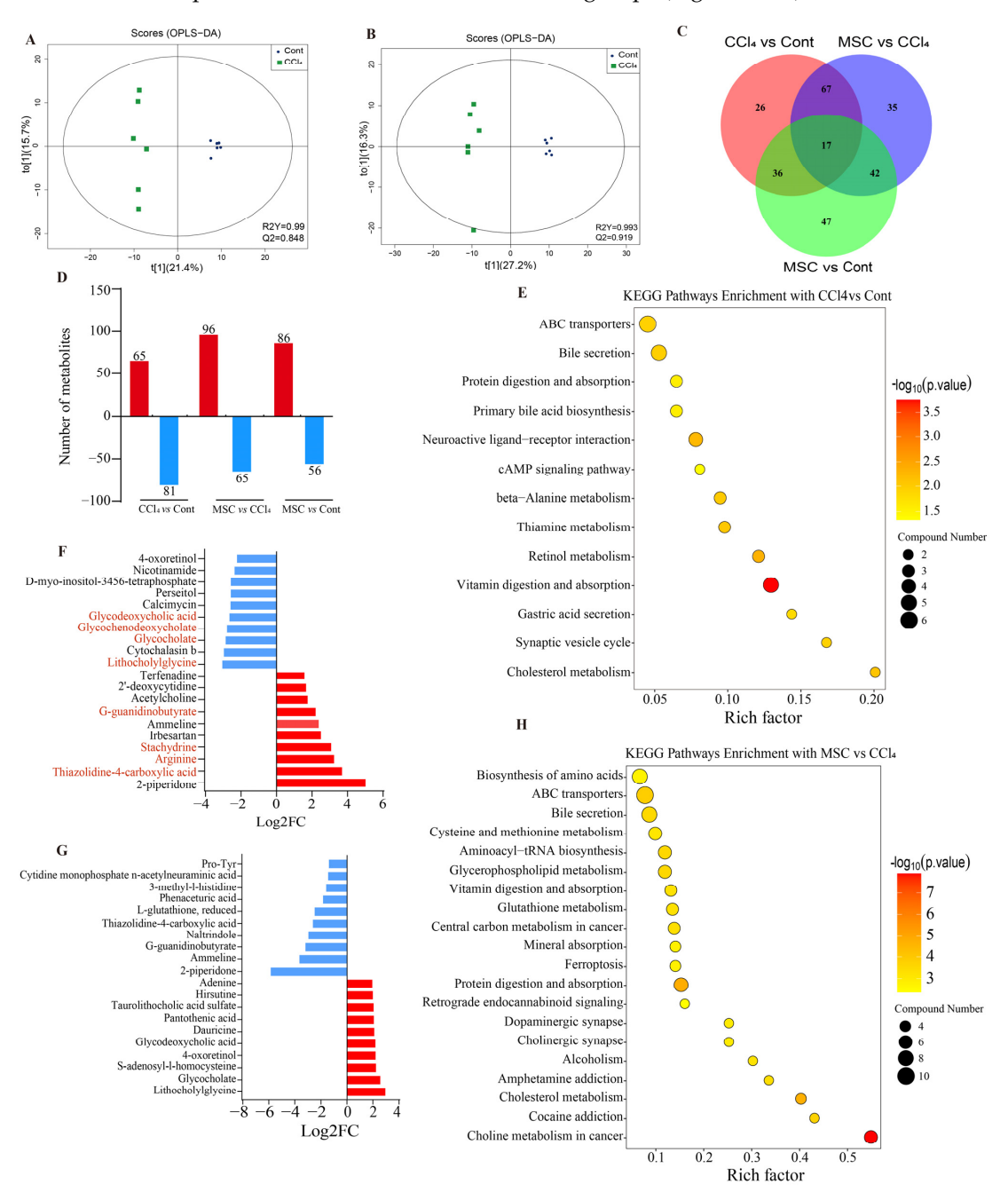


Figure 2. Changes in the liver metabolic profile in CCl₄-induced LF rats and ADMSCs transplantation rats. (**A**) OPLS-DA score plot of liver metabolites after intraperitoneal CCl₄ injection; (**B**) OPLS-DA score plot of liver metabolites after ADMSCs transplantation; (**C**) VEEN plot of the number of DMs in rat livers obtained via a pairwise comparison between Cont, CCl₄, and MSC groups; (**D**) Number of DMs up- and downregulated in liver tissues revealed via pairwise comparisons; (**E**,**F**) Top 10 up- and downregulated DMs and KEGG enrichment of CCl₄ vs. Cont; (**G**,**H**) Top 10 up- and downregulated DMs and KEGG enrichment in MSC vs. CCl₄; Cont, control group; CCl₄, CCl₄-treated group; MSC, ADMSCs-treated group; DMs, differently expressed metabolites.

Int. J. Mol. Sci. 2023, 24, 16086 5 of 17

In all three experimental groups, six biological repeats were conducted, resulting in the identification of 267 DMs (Figure 2C). These findings suggest that there are significant differences in metabolic status among the groups. The present study identified significant differential metabolites in the liver tissue of Cont, CCl₄, and MSC rats using pairwise comparisons. It was found that, compared to the Cont group, the CCl₄ and MSC groups had 146 (65 up- and 81 downregulated) and 142 (86 up- and 56 downregulated) DMs in the liver tissue, respectively. Additionally, the CCl₄ and MSC groups had a total of 161 (96 up- and 65 downregulated) DMs in the liver tissue (Figure 2D). This study found that there are 84 types of DMs expressed in both Cont vs. CCl₄ as well as MSC vs. CCl₄ with opposite trends (Supplementary Table S1). These findings indicate that the treatment of ADMSCs may have the ability to reverse some of the biological functions that are damaged by CCl₄.

In order to reveal the specific mechanism of ADMSCs participating in the treatment of LF, the KEGG dataBAe was used to conduct pathway enrichment analysis on DMs in three groups. The top 10 metabolites up- and downregulated in CCl₄ vs. Cont and MSC vs. CCl₄ are shown in Figure 2F,G. Compared with the Cont group, 4 of the top 10 up-regulated metabolites belong to amino acids (Thiazolidine-4-carboxylic acid, Arginine, Stachydrine and G-guanidinobutyrate) and 4 of the top 10 downregulated metabolites belong to BA (Lithocholylglycine, Glycocholate, Glycochenodeoxycholate and Glycodeoxycholic acid) (Figure 2F) in CCl₄ group. As two markers of bile secretion, the expression of Glycocholate and Glycochenodeoxycholate in CCl₄ vs. Cont decreased significantly. After MSC treatment, this trend was reversed (Figure 2F,G). According to the *p*-value of KEGG enrichment (Figure 2E,H), it was found that most DMs are closely related to the metabolism and secretion of the bile pathway, including mainly retinol metabolism, primary bile biosynthesis, cholesterol metabolism, and beta-Alanine metabolism, etc.

2.3. Changes in Liver Transcriptome after Adipose Mesenchymal Stem Cell Transplantation

RNA sequencing (Rna-Seq) technology was used to detect the gene expression in liver tissues of the Cont group, CCl₄ group, and MSC group. Sequencing data were quality-controlled and annotated, and all sequencing results matched more than 95% of the reference genome (Supplementary Table S2). Principal component analysis (PCA) showed that the gene pattern of rats in the CCl₄ group was clearly separated from the remaining two groups. In addition, we found similar gene expression patterns in the liver of rats in the Cont and MSC group (Figure. 3A). A total of 4751 DEGs were identified through pairwise comparison (Figure 3B and Supplementary S2). Compared with Cont rats, 3669 genes (2286 upregulated and 1383 downregulated) and 1112 genes (925 upregulated and 187 downregulated) were differentially expressed in CCl₄ and MSC rats, respectively. In addition, 2747 DEGs (1185 upregulated and 1562 downregulated) were observed between CCl₄ and MSC rats (Figure 3C–E).

The pathway enrichment analysis of detected DEGs was conducted BAed on the KEGG dataBAe. According to the p-value of KEGG enrichment, the metabolism of xenobiotics via cytochrome P_{450} , drug metabolism cytochrome P_{450} , steroid hormone biosynthesis, fatty acid degradation, the PPAR signaling pathway, Retinol metabolism, tryptophan metabolism, and butanoate metabolism are the common pathways of CCl_4 and ADMSCs. Primary BA biosynthesis and bile secretion were enriched, which further proves that the liver function of ADMSCs is related to bile homeostasis (Figure 3F,G).

2.4. Alterations of Genes and Metabolites Related to Primary BA Biosynthesis and Bile Secretion

In order to further elucidate the relationship between the two omics results, conjoint analysis was conducted BAed on the KEGG enrichment results, with the most important being the synthesis of primary BA and bile secretion. As shown in Figure 4A,C, compared to Cont and CCl₄, the DMs and DEGs present in these two pathways in MSC exhibited similar and almost opposite expression trends, indicating that ADMSCs may treat LF by regulating the primary BA biosynthesis and bile secretion disturbances caused by CCl₄.

Int. J. Mol. Sci. 2023, 24, 16086 6 of 17

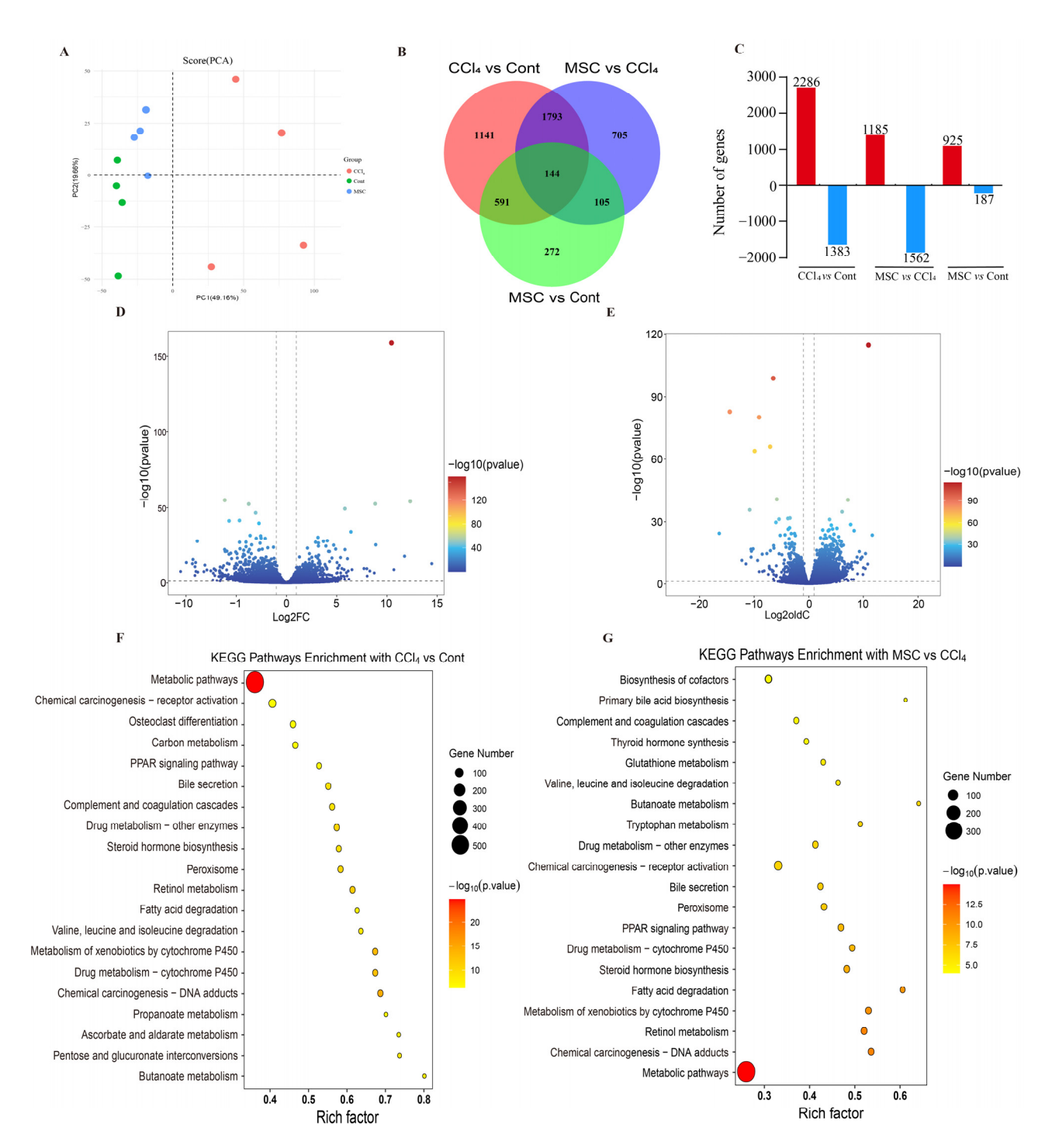


Figure 3. Changes in the liver transcriptional profile in CCl₄-induced LF rats and ADMSCs transplantation rats. (**A**) PCA score plots of liver tissues of the three groups of rats; (**B**) VEEN plot of the number of DEGs in rat livers obtained via pairwise comparison between Cont, CCl₄, and MSC groups; (**C**) Number of DEGs up- and downregulated in liver tissues revealed via pairwise comparisons; (**D**,**E**) Volcano plot of differential genes in CCl₄ vs. Cont and MSC vs. CCl₄; (**F**) Significantly enriched KEGG pathways in the CCl₄ vs. Cont comparison; (**G**) Significantly enriched KEGG pathways in the MSC vs. CCl₄ comparison. Cont, control group; CCl₄, CCl₄-treated group; MSC, ADMSC₅-treated group; DEGs, differently expressed genes.

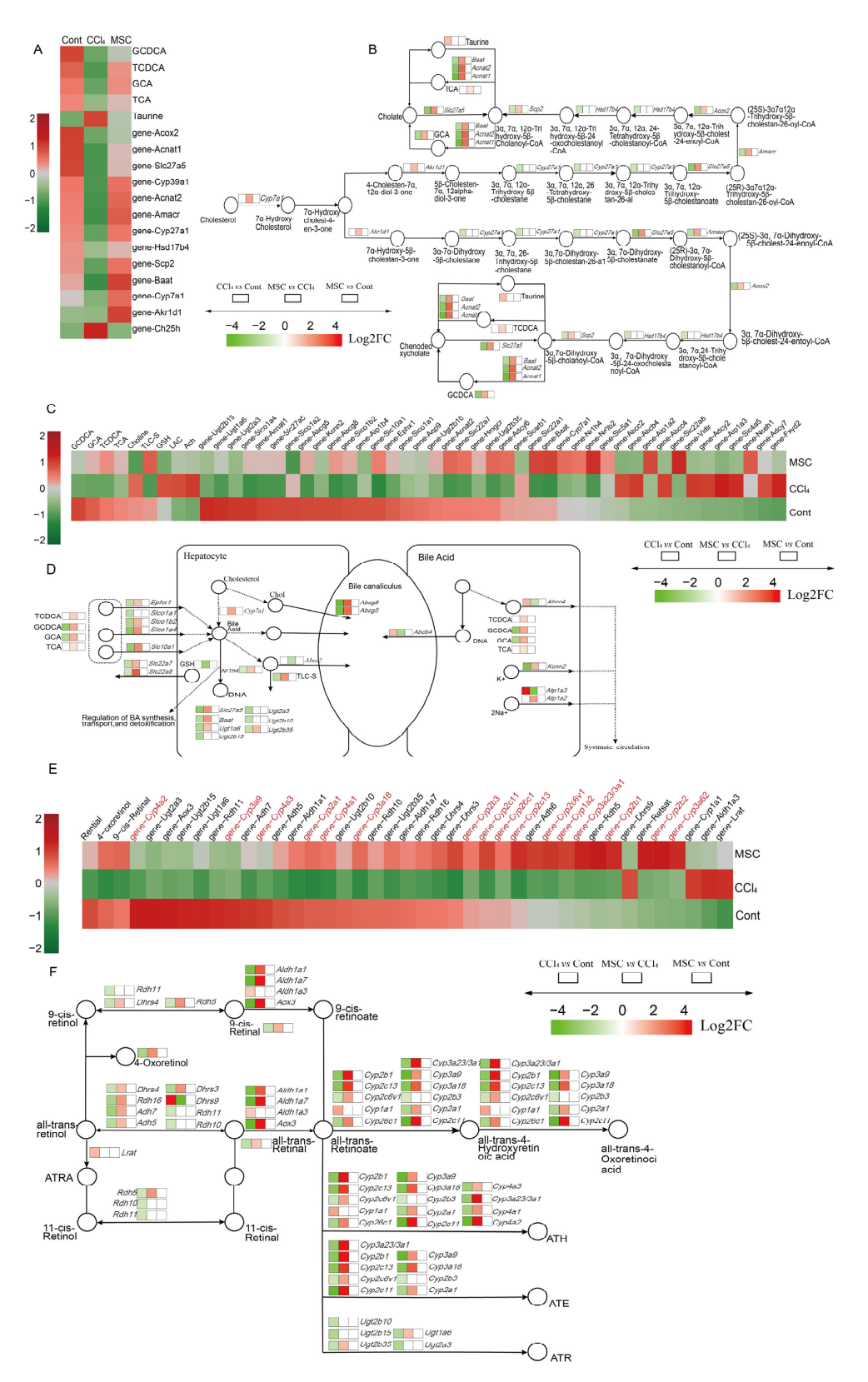


Figure 4. Effects of ADMSCs on genes and metabolites involved in primary BA synthesis, bile secretion, and retinol metabolism pathways. (**A**,**C**,**E**) Heatmaps of DMs and DEGs expression associated with primary BA biosynthesis, bile secretion, and retinol metabolism; (**B**,**D**,**F**) The most relevant metabolites and differentially expressed genes perturbed by CCl₄ and reversed by ADMSCs in primary BA biosynthesis, bile secretion, and retinol metabolism pathway. DMs, differential metabolites; DGEs, differentially expression genes.

An important BA, Glycochenodeoxycholic acid (GCDCA), was downregulated in rats with LF because the genes Slc27a5, Amacr, Acox2, Scp2, Baat, Acnat1, and Acnat2 involved in primary BA synthesis were all downregulated (Figure 4A,B). The expression of Cyp7a1 and Akr1d1 was not significantly downregulated in rats with hepatic fibrosis, but this trend was significantly reversed after the transplantation of ADMSCs (Figure 4B). Cyp27a1 and Hsd17b4 have opposite trends to the two genes described above. After ADMSCs treatment, not only did the expression of GCDCA and GCA increase, but two important BA, Taurochenodeoxycholic acid (TCDCA) and Taurocholic acid (TCA), were also detected but were not found in CCl₄ vs. Cont (Figure 4B). When the bile secretion pathway was activated after primary BA synthesis, the four representative primary BA were transported to hepatocytes. At the same time, the expression levels of genes Slco1b2, Slco1a4, Slc10a1, and *Ephx1* in MSC vs. CCl₄ were increased (Figure 4D). BA maintain cholesterol balance. The increased expression of Cyp7a1 after the transplantation of ADMSCs accelerated the conversion of cholesterol to BA, and the upregulation of Nr1h4 promoted the synthesis, transport, and detoxification of BA (Figure 4C). The genes Nr1h4, Slc27a5, Ugt1a6, Ugt2b35, and Baat, which alleviate BA toxicity, were upregulated in the MSC group (Figure 4D). Meanwhile, the increased expression of Abcg8, Abcg5, and Abcc2 in the MSC group promoted the excretion of BA into bile ducts (Figure 4D).

2.5. Alterations of Genes and Metabolites Related to Retinol Metabolism

In addition to primary BA synthesis and bile secretion, retinol metabolism also plays an important role in the regulation of metabolic disorders caused by CCl_4 -induced LF [27]. There are three important retinol metabolites, Retinal, 4-Oxoretinol, and 9-cis-Retinal, which are downregulated in CCl_4 vs. Cont, while in MSC vs. CCl_4 , their expression is upregulated, suggesting that ADMSCs may treat CCl_4 -induced LF by promoting retinol metabolism (Figure 4E,F). Genes associated with retinol metabolism showed similar expression patterns in Cont and MSC. Figure 4E shows that, among the genes most related to retinol metabolism, there were 17 genes belonging to the cytochrome P_{450} family-1,2,4,3,26, all of which played important roles in retinol metabolism.

2.6. Correlations between DGEs and DMs Related to Primary BA Biosynthesis, Bile Secretion and Retinol Metabolism

BAed on these aforementioned findings, it can be observed that the regulation of a metabolite can be influenced by a diverse array of genes, subsequently impacting and controlling various pathways. Consequently, the association between DEGs and DMs holds significant importance for the identification of subsequent biomarkers. To this end, we involved a correlation network of primary BA synthesis, bile secretion, and retinol metabolism pathways in MSC vs. CCl₄. Notably, all DEGs and DMs included in the network diagrams exhibited correlations exceeding 0.7 and possessed statistical significance.

A total of 35 genes and 8 metabolites were identified that jointly regulated the primary BA biosynthesis and BA secretion pathways (Figure 5A). Among these genes, *Acox*2 was specifically related to TCDCA. Furthermore, GCDCA is associated with *Slc27a5*, *Baat*, and *Slc01a4*, while GCA is linked to *Cyp7a1*, *Abcb4*, *Akr1d1*, and others. These associations suggest that multiple genes may co-regulate the aforementioned metabolites. In addition, retinol metabolism, as a key pathway in LF, is regulated at the transcriptional level via ADMSCs, where *Ugt2b35*, *Cyp3a18*, *Cyp2c13*, *Retsat*, *Adh7*, and *Dhrs4* are related to the metabolic markers 4-Oxoretinol, Retinal, and 9-cis-Retinal (Figure 5B).

2.7. Candidate Gene Validation

Subsequently, the expression levels of seven key genes involved in BA biosynthesis, bile secretion, and retinol metabolism were verified through qPCR and Western blotting (Figure 6). The primers for these seven genes are listed in Table 1. Notably, the expression levels of these genes decreased after CCl₄ intervention but were significantly upregulated following the treatment of ADMSCs. It is interesting that the expression levels of these

genes in the liver tissue of rats treated with ADMSCs were higher than those in the Cont group, and there was a statistical difference compared to the expression levels of related genes in CCl₄. Overall, these results are consistent with transcriptome sequencing findings, suggesting that ADMSCs play a therapeutic role in regulating the expression of key genes in relevant pathways.

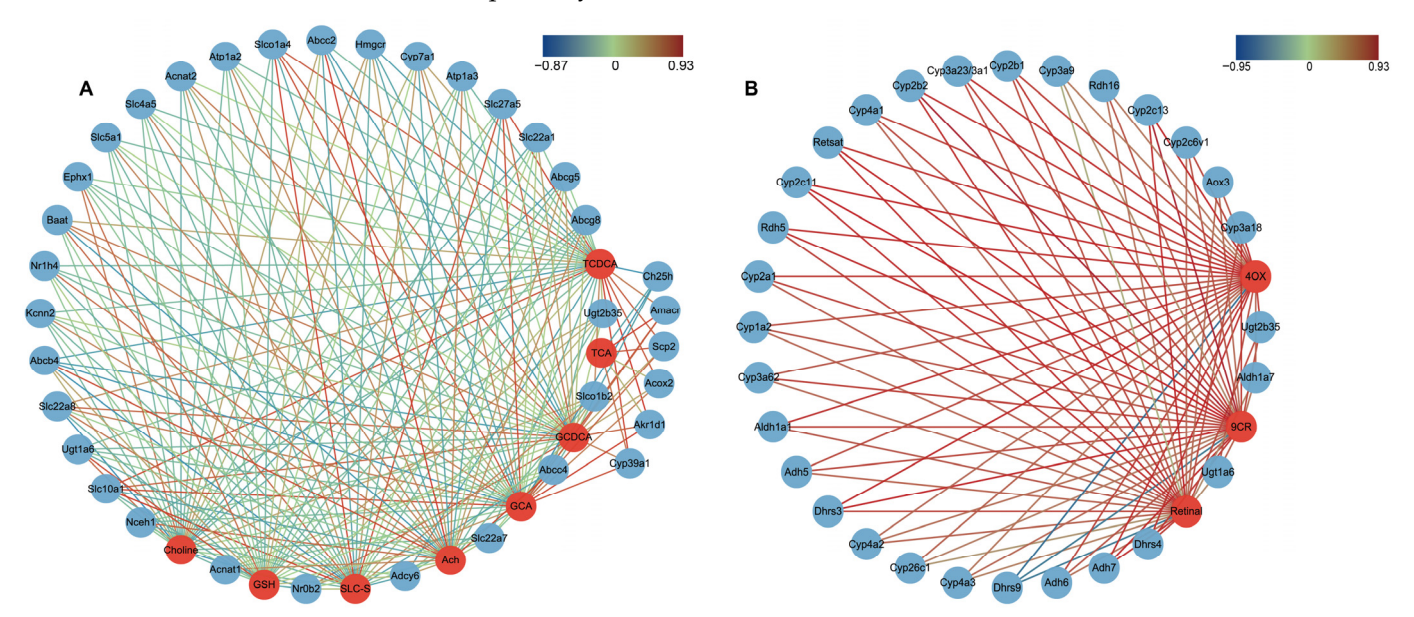


Figure 5. Correlation network analysis. (**A**) Correlation analysis of primary BA synthesis and bile secretion; (**B**) Correlation analysis of retinol metabolism. Red circles are DMs, and blue circles are DEGs. DMs, different expressed metabolites. DEGs, different expressed genes; TCDCA, Taurochenodeoxycholic acid; GCDCA, Glycochenodeoxycholic acid; GCA, glycocholic acid; TCA, Taurocholic acid; TLC-S, Taurolithocholic acid 3-sulfate; GSH, Glutathione; Ach, Acetylcholine; 9CR, 9-cis-Retinal; 4OX, 4-Oxoretinol.

Table 1. Primers used for qPCR.

Gene	Primer Sequence (5-3')	bp
<i>Cyp7a1-</i> Forward	CTGCCGGTACTAGACAGCAT	20
Cyp7a1-Reverse	TCCTCCTTAGCTGTGCGGAT	20
Сур27а1	GGAACAGGTCAAGACCGACC	20
Cyp27a1	CTTGTTCAGCGCCTGGAG	18
Adh7	TGGGCCAGTTGATAACCCAC	20
Adh7	GGACAGTCCGAATGCTTTGC	20
Baat	CTGTCGAACTACGGTTTTGGC	21
Baat	GCTGTCAGCTTGGCCATTTT	20
Retsat	CATTCTGCCGAGCGTCTACT	20
Retsat	GCTGGGGGTTACTCCGTAAG	20
Slco1a4	AGCTTCTTCATAAAAACAGCAGTAA	25
Slco1a4	TGTTAATGCCAACAGAAACATCTTG	25
Dhrs4	CTTGGCACCTGGACTCATCA	20
Dhrs4	CTGGCTTGCCTAGCCTTCTA	20
GADPH	ACAGCAACAGGGTGGTGGAC	20
GADPH	TTTGAGGGTGCAGCGAACTT	20

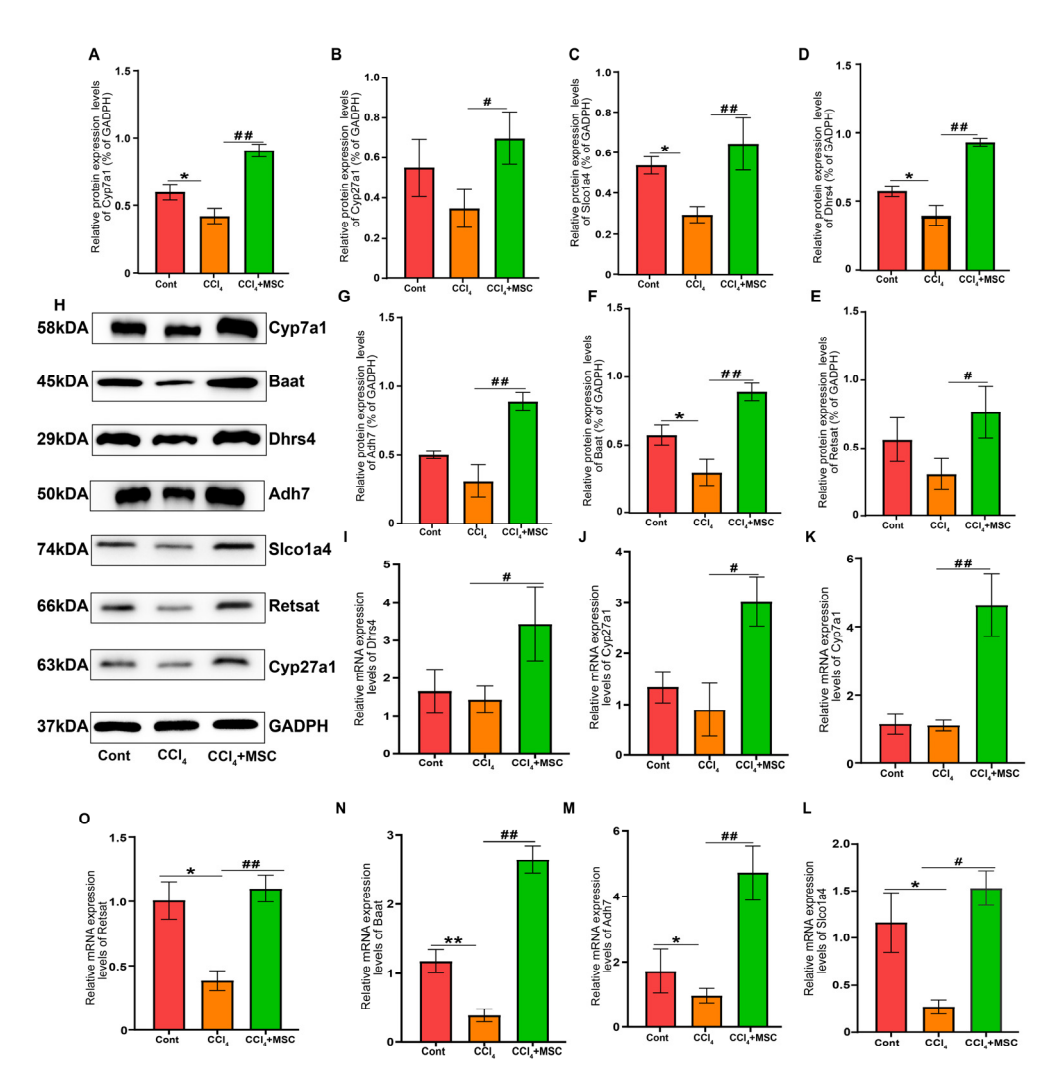


Figure 6. q-PCR and Western blot validation of 7 candidate genes. (**A–G**) The levels of *Cyp7a1*, *Cyp27a1*, *Baat*, *Dhrs4*, *Adh7*, *Slco1a4*, and *Retsat* mRNA expression in each group; (**H–O**) The levels of *Cyp7a1*, *Cyp27a1*, *Baat*, *Dhrs4*, *Adh7*, *Slco1a4*, and *Retsat* protein expression in each group. Each experiment was carried out at least three times, and data are displayed using mean \pm SD. Cont, control group; CCl₄, CCl₄ intervention group; MSC, ADMSCs treatment group. *, *p* < 0.05; **, *p* < 0.01 vs. Cont group; #, *p* < 0.05; ##, *p* < 0.01 vs. MSC group.

3. Discussion

LF, a wound-healing response, is a common occurrence in various liver injuries and poses a significant threat to both human and animal health. One highly toxic compound, CCl₄, is known to cause liver necrosis and release proinflammatory and fibrotic cytokines, thereby leading to LF and potentially cirrhosis [28]. Several studies have indicated that a disruption in the metabolism of BA (BA) can contribute to liver injury and fibrosis. Various interventions, such as inhibiting toxic BA levels and regulating BA homeostasis using Taurocholic acid and the probiotic Lactobacillus rhamnosus GG, have shown promising results in improving liver injury and fibrosis in mice [29]. While ADMSCs have shown therapeutic effects on CCl₄-induced liver injury models [30,31], it is still unclear how they exert these effects by regulating metabolic levels in the body. This study aims to identify and analyze the metabolic and transcriptional products of liver tissues in rats with CCl₄-induced LF and investigate the specific mechanism through which ADMSCs treat LF.

BA (BA) are amphiphilic molecules that are produced through the metabolism of cholesterol in the liver. They make up over 50% of the organic matter in bile, and their synthesis and secretion pathways are intricately regulated. BA consist of the following two components: primary BA, which are produced directly by hepatocytes, and secondary BA,

which are formed after being secreted into the intestine [32,33]. Secondary BA synthesized in the intestine are absorbed via the liver through the hepatic portal vein, playing a crucial role in maintaining the balance of bile flow in the body. In the liver, these BA contribute to the clearance of endogenous compounds and metabolites, such as bilirubin and hormones, as well as exogenous substances like drugs. Moreover, BA serve as signaling molecules that regulate lipid, glucose, and energy metabolism in the liver. They achieve this by interacting with the BA receptor, FXR, and takeda G protein-coupled receptor 5 (TGR5). Furthermore, secondary BA in the intestine play a significant role in controlling cell proliferation and inflammatory responses in both the liver and intestine. This is achieved through the absorption of lipophilic nutrients into the intestine [33]. The occurrence of a variety of liver diseases is accompanied by the disorder of BA metabolism [34,35]. In the CCl₄-induced liver injury model, the synthesis, secretion, and reabsorption of BA are disrupted, leading to the increased expression of total bile acid (TB) in the liver and promoting the progression of LF [36,37]. Studies have found that the accumulation of BA in hepatocytes accelerates the progression of NASH by promoting ER stress and de novo fat synthesis. In HFDinduced NAFLD, researchers found that the expression of Ursodeoxycholic acid (UDCA) and Taurohyodeoxycholic acid (THDCA) in the liver was significantly decreased [38]. In addition, the gut microbiota-mediated inactivation of the FXR-FGF15 axis was observed in patients with primary-sclerosed cholangitis (PSC) due to cholestasis, resulting in the persistently elevated content of BA in the liver through the negative feedback regulation of BA' synthesis inhibition [39]. In dimethylnitrosamine (DMN)-induced LF, the expression of TCDCA, GCDCA, GCA, and TCA in the liver was significantly reduced [40]. TCDCA has the ability to resist cell apoptosis and reduce endoplasmic reticulum stress and has demonstrated its therapeutic potential in experimental acute liver injury induced by excessive acetaminophen (APAP) [41]. When the content of GCDCA is decreased, the presence of cholestatic liver disease is often suggested [42]. In this study, the four BA detected were TCDCA, GCDCA, TCA, and GCA, all of which belong to primary BA. This indicates that ADMSCs mainly exert therapeutic effects by affecting the synthesis of primary BA.

BA are primarily produced in the liver through two enzymatic pathways as follows: the classical or neutral synthesis pathway, which involves the rate-limiting enzyme Cyp7a1 [43], and the acidic or remedial pathway, initiated by Cyp27a1 [44]. The inhibition of either pathway results in impaired bile flow in the body. It is important to note that in rats with LF, the expression of *Cyp27a1* is significantly reduced. However, after treatment with ADMSCs, the expression of *Cyp7a1* is significantly increased. This suggests that CCl₄ may hinder the synthesis and secretion of BA by inhibiting the alternative pathway of bile synthesis, while ADMSCs promote stable bile flow by enhancing the classical synthesis pathway. Slco1a4, as a member of the OATP family, is involved in the liver's absorption of free secondary BA from the blood [45]. The Solute Carrier Family 27 Member 5 gene (Slc27a5) is a member of the Slc27a gene family and encodes the fatty acid (FA) transport protein 5 (*Fatp5*). This protein plays a crucial role in FA transport and BA metabolism. Studies have shown that *Slc27a5* knockout mice have reduced FA intake, accompanied by liver injury, insulin resistance, and dyslipidemia [46,47]. The primary free BA (CDCA, CA) produced by the liver needs to be conjugated with glycine or taurine to become primary conjugated BA (TCDCA/GCDCA/TCA/GCA), which enters the intestine. This process is regulated by Baat and is often accompanied by a decrease in Baat expression in cholestatic liver diseases [48,49]. Previous research indicates that MSCs upregulate the expression of Slc27a5 and Baat, promoting the synthesis and secretion of BA, as well as lipid reabsorption. Additionally, *Abcg5* and *Abcg8*, which are part of the ATP-binding box (ABC) transporter family, play a crucial role in promoting cholesterol excretion into bile in hepatocytes [50]. Another metabolite involved in these pathways is Glutathione (GSH), which has been reported to regulate sterol balance by affecting the activity of Cholesterol 7 alpha-hydroxylase (CH-7 alpha) [51].

The activation of hepatic stellate cells plays a pivotal role in the progression of LF, as their transition into myofibroblast-like cells serves as the primary mechanism for the

deposition of the ECM. These cells also serve as an important reservoir for vitamin A, and their activation can result in the significant depletion of this essential nutrient. Vitamin A encompasses biologically active compounds such as retinol and its metabolites, including Retinal, 9-cis-retinal (9cRAL), and 4-oxidized retinol, which were identified in this study. Vitamin A plays an important role in the body's vision, growth [52], reproduction, immune function [53], and metabolic processes. The genes *Adh7*, *Rdh5*, *Retsat*, and *Aldh1a1*, which play a crucial role in the metabolic pathway of vitamin A [54], specifically, Adh7 and *Aldh1a1*, facilitate the transformation of retinol into its biologically active form, retinoic acid (RA) [55]. Many studies have shown that liver cells in vitamin A-deficient rats show obvious vacuolization, steatosis, and mild inflammatory infiltration [56]. In addition, it was found that the progression of LF was negatively correlated with liver RA content. Vitamin A enters the liver only through the transport of secondary BA in the intestine. Studies have shown a correlation between VAD, cholestasis, and fibrosis in patients. This association can be attributed to two primary factors. First, reduced bile flow from the liver leads to lower concentrations of BA in the gut, which hinders the absorption of vitamin A. Second, alterations in the gut microbiota prevent the hepatic uptake of secondary BA by inhibiting FXR signaling. In our study, we found that the synthesis of four primary BA (TCDCA, GCDCA, TCA, and GCA) was inhibited in CCl₄-induced fibrosis rats, while the levels of retinol-related secondary metabolites were significantly reduced. However, the demyelination trend was reversed after the transplantation of ADMSCs. These findings indicate that ADMSCs may possess therapeutic properties by suppressing HSC activation and enhancing bile flow, ultimately facilitating the absorption of vitamin A.

BAed on the results of this experiment, we found that ADMSCs promote the synthesis and secretion of TCA, GCA, TCDCA, GCDCA, and GSH. Additionally, they enhance the expression of key genes (*Cyp7a1*, *Cyp27a1*, *Abcg5*, *Abcg8*, *Baat*, and *Slc27a5*) associated with these metabolites, thereby promoting sterol balance and bile secretion in the body. On the other hand, ADMSCs upregulate the expression of key genes such as *Adh7*, *Slco1a4*, *Aldh1a1*, *Retsat*, and *Dhrs4*, which helps maintain the stability of Retinal, 9-cis retinol, and 4-Oxoretinol in the liver. This inhibits the activation of hepatic stellate cells and promotes an immune response, leading to therapeutic effects.

4. Materials and Methods

4.1. Animal Treatment and Sample Collection

Eighteen male Sprague Dawley rats, 4 weeks old, weighing 200–220 g, were purchased from the Dashuo Experimental Animal Company (Chengdu, China). After one week of adaptive feeding, we randomly divided them into the following three groups: Cont (control group), CCl₄ (CCl₄ intervention group), and MSC (ADMSCs treatment group), with six rats in each group. This study complied with the guidelines for the Care and Use of Laboratory Animals by the National Institutes of Health. This study was approved by the Sichuan Agricultural University Institutional Animal Care and Use Committee (No. SYXK 2019-187).

The control group, the CCl₄ intervention group and ADMSCs treatment group were treated as follows: control group, intraperitoneal injection of olive oil 2 mL/kg twice a week for 4 weeks; CCl₄ intervention group, intraperitoneal injection of CCl₄ (2 mL/kg) mixed with olive oil solution (v:v/4:6) twice a week for 4 weeks; ADMSCs treatment group, 24 h after the last intraperitoneal injection of CCl₄-olive oil solution, ADMSCs (1.5×10^6 ADMSCs dissolved in 0.5 mL PBS solution) were transplanted via the tail vein once a week for 1 week. At the end of the animal experiment, and after fasting for 24 h, rats were anesthetized with sodium pentobarbital, and the liver and venous serum samples were collected. Serum samples were used to determine biochemical markers of liver function, and tissue samples were frozen in liquid nitrogen and stored at -80 °C for subsequent experiments.

4.2. Serum Biochemical and Inflammatory ELISA Factor Analysis

After blood collection from the abdominal aorta, it was immediately placed in a $4\,^{\circ}$ C ice box for one hour. Subsequently, the blood sample was centrifuged at $4\,^{\circ}$ C and $5000\,\text{r/mp}$ for 20 min to obtain the serum. The levels of ALT, AST, TBIL, and GGT were then measured using the IDXX Biotechnology Co., Ltd. (Westbrook, Maine, USA) kit. The expression levels of inflammatory factors IL-6 and TNF- α were measured according to the manufacturer's instructions (Ke Xing, Shanghai, China).

4.3. Histological and Immunohistochemistry Analysis

Liver tissue was fixed by 4% Paraformaldehyde at 4 $^{\circ}$ C for 24 h, then paraffin-embedded liver tissue was dehydrated and cut into 5 μ m sections for HE and MASSON staining. The immunohistochemical determination of α -SMA expression in liver tissue was performed on the remaining embedded tissues. ImageJ software (V1.8.0.112) was used for the quantitative analysis of collagen fibers and α -SMA in MASSON and immunohistochemistry.

4.4. Transcriptomic Analysis

The total RNA was extracted from the liver using TRIzol (Magen, Shanghai, China). RNA samples were detected BAed on the A260/A280 absorbance ratio with a Nanodrop ND-2000 system (Thermo Scientific, Rockford, IL, USA), and the RIN of RNA was determined using an Agilent Bioanalyzer 4150 system (Agilent Technologies, Santa Clara, CA, USA). Only qualified samples were used for library construction. Paired-end libraries were prepared using a ABclonal mRNA-seq Lib Prep Kit (ABclonal, Wuhan, China). Library quality was assessed on an Agilent Bioanalyzer 4150 system, and the library preparations were sequenced on an Illumina Novaseq 6000. The original data were filtered via Q30, and low-quality fragments were eliminated using fastp software (v0.17.0). (The clean reading was then compared with the rat reference genome using HISAT2 (v2.1.0) (http://daehwankimlab.github.io/hisat2/ (accessed on 15 June 2023)) software, and all subsequent analyses were conducted on the clean reading; the FPKM algorithm was used to quantify gene expression levels. Genes with |log₂FC| > 1 and Padj < 0.05 were considered DEGs. DEGs were then used for gene ontology (GO) function analysis and the Kyoto Encyclopedia of Genes and Genomes (KEGG) pathway analysis.

4.5. Metabolomic Analysis

We then added 200 μL of ddH₂O to 80 mg of liver tissue for the preparation of the tissue homogenate while adding 800 μ L of methanol/acetonitrile (1:1, v/v) to the homogenate. This was then centrifuged for 20 min (14,000× g, 4 °C) before the supernatant was dried in a vacuum centrifuge. The obtained dried substance was remelted in 10 µL of solvent acetonitrile/water (1:1, v/v), centrifuged for 15 min (14,000× g, 4 °C), and the supernatant was taken and loaded into a dedicated vial for UHPLC-MS/MS analysis. The samples were separated on an Agilent 1290 Infinity LC system (UHPLC)HILIC column. The specific parameters were as follows: was column temperature was 25 °C; the flow rate was 0.5 mL/min; and the injection volume was 2 μL. Mobile phase composition A was as follows: water +25 mM ammonium acetate +25 mM ammonia water, B: acetonitrile. The gradient elution procedure was as follows: 0–0.5 min, 95% B. From 0.5 to 7 min, B changed linearly from 95% to 65%. From 7 to 8 min, B changed linearly from 65 to 40%. At 8–9 min, B was maintained at 40%. From 9 to 9.1 min, B changed linearly from 40 to 95%. At 9.1-12 min, B was maintained at 95%. The samples were placed in an autosampler at 4 °C throughout the analysis. QC samples were randomly inserted into the assay to monitor the reliability of the system and experimental data. Subsequent mass spectrometry was performed on a Triple TOF 6600 mass spectrometer using electrospray ionization (ESI) in positive ion and negative ion modes. Ion source, turbo spray; source temperature, 500 °C; ion spray voltage floating (ISVF) ± 5500 V; Gas1, Gas2, and CUR were set at 60 psi, 60 psi, and 30 psi, respectively. The primary mass-to-charge ratio detection range was 60 to 1000 Da, the scan cumulative time was 0.20 s/spectra, the detection range of

the second-order daughter ion mass-to-charge ratio was 25–1000 Da, and the scanning accumulation time was 0.05 s/spectra.

4.6. Data Processing and Annotation

Progenesis XCMS software (v 4.0.0) was used for LC-MS data extraction, alignment, peak picking, and retention time adjustment. The company's own library with the standard mass spectra on the commercial dataBAes was compared using mzCloud (https://www.mzcloud.org (accessed on 20 May 2023)), HMDB (http://www.hmdb.ca (accessed on 20 May 2023)), and KEGG (http://kegg.jp (accessed on 22 May 2023)), All metabolites were identified by "score", "fragment score", "mass error (ppm)" and "isotopic similarity" [57].

4.7. Statistical Analysis

Data were represented as the mean \pm standard deviation. The double-tailed student t-test, one-way analysis of variance (ANOVA), and Bonferroni post-tests were performed. PCA and orthogonal partial least squares discriminant analysis (OPLS-DA) were used to analyze metabolomic data. Permutation tests were conducted to ensure the stability of the model. The importance of each variable in the projection (VIP) value of the OPLS-DA model was calculated to indicate its contribution to classification. Metabolites with VIP > 1 and p < 0.05 were considered as significantly different metabolites (DMs). The Pearson correlation coefficient was used to explain the correlation between these two variables. Differential metabolites were then summarized and mapped to biochemical pathways using KEGG enrichment analysis. The pathways of significant enrichment were identified using Fisher's precise test.

4.8. Validation of DEGs by qPCR and Western Blot

The total RNA was extracted from the liver using an animal total RNA isolation kit (Foregene, Chengdu, China). The cDNA was reverse transcribed using the FastKing-RT SuperMix kit (Tiangen, Beijing, China) according to the manufacturer's protocol. In addition, qPCR was performed using the BioRad Laboratories CFX ConnectTM real-time PCR Detection System. The housekeeping gene GADPH was used for the normalization of the data. The results were quantified using the $2^{-\Delta\Delta Ct}$ method relative to the housekeeping gene actin. The sequences of the primers used are placed in Table 1.

Liver tissue homogenates were sonicated to dissolve completely and then centrifuged at 12,000 rpm for 30 min at 4 °C to separate the membrane-containing fraction (pellet) from the cytosol. Proteins (100 μ g) were separated by 10% SDS-polyacrylamide gel electrophoresis. The separated proteins were transferred onto a nitrocellulose membrane (NC membrane, Millipore, Billerica, MA, USA), washed for 10 min with TBST, and then immersed in a blocking buffer containing 5% nonfat dry milk in TBST for 1 h at room temperature. The membrane was washed with TBST and incubated overnight at 4 °C with polyclonal primary antibodies Dhrs4 (Abcam, Cambridge, UK) diluted 1:2000, Baat (Abcam) and Cyp7a1 (Proteintech Group, Inc., Chicago, IL, USA) diluted 1:500, and Adh7 (Shanghai-Youke Biotechnology, Inc., Shanghai, China) diluted at 1:1000 in 5% nonfat dry milk. Then, the membrane was incubated with a secondary antibody (Cell Signaling Technology, Danvers, MA, USA) for 1h at room temperature. Finally, the membrane was scanned using the Odyssey Infrared Imager (LI-COR, Lincoln, NB, USA), and the bands were quantified by densitometry using Odyssey software (version 1.2, LI-COR).

5. Conclusions

The research results show that ADMSCs have therapeutic effects on LF induced by CCl₄. The joint analysis of transcriptome and metabolomics revealed that ADMSCs accelerated the synthesis and secretion of primary BA (TCDCA, GCDCA, GCA, and TCA) by promoting gene expression such as *Cyp7a1*, *Baat*, *Cyp27a1*, *Adh7*, and *Slco1a4*, maintaining the body's BA homeostasis and correcting vitamin A metabolism disorders, thus

exerting therapeutic effects. The discovery of these new biomarkers in metabolomics and transcriptomics could provide new drug discovery and therapeutic strategies for LF.

Supplementary Materials: The supporting information can be downloaded at: https://www.mdpi.com/article/10.3390/ijms242216086/s1.

Author Contributions: Conceptualization, H.L.; Data curation, D.C.; Formal analysis, X.W. and X.M.; Funding acquisition, H.L. and D.C.; Methodology: S.C.; Project administration, H.L. and Z.Z. (Ziyao Zhou); Resources, Y.L.; Software, X.W. and H.D.; Supervision, G.P.; Validation and X.W.; Visualization, Z.Z. (Zhijun Zhong) and L.S.; Writing—original draft, X.W.; Writing—review and editing, G.P. and H.H. All authors have read and agreed to the published version of the manuscript.

Funding: This research was funded by the National Natural Science Foundation of China (32002353) and the Natural Science Foundation of Sichuan Province (2022NSFSC1680).

Institutional Review Board Statement: Not applicable.

Informed Consent Statement: Not applicable.

Data Availability Statement: The data used to support the findings of this study are available from the corresponding author upon request.

Conflicts of Interest: There are no conflicts of interest according to the authors.

References

- 1. Hernandez-Gea, V.; Friedman, S.L. Pathogenesis of liver fibrosis. Annu. Rev. Pathol. 2011, 6, 425–456. [CrossRef] [PubMed]
- 2. Seki, E.; Brenner, D.A. Recent advancement of molecular mechanisms of liver fibrosis. *J. Hepato-Biliary-Pancreat. Sci.* **2015**, 22, 512–518. [CrossRef] [PubMed]
- 3. Meng, F.; Wang, K.; Aoyama, T.; Grivennikov, S.I.; Paik, Y.; Scholten, D.; Cong, M.; Iwaisako, K.; Liu, X.; Zhang, M.; et al. Interleukin-17 signaling in inflammatory, Kupffer cells, and hepatic stellate cells exacerbates liver fibrosis in mice. *Gastroenterology* **2012**, *143*, 765–776.e3. [CrossRef] [PubMed]
- 4. Ding, B.S.; Cao, Z.; Lis, R.; Nolan, D.J.; Guo, P.; Simons, M.; Penfold, M.E.; Shido, K.; Rabbany, S.Y.; Rafii, S. Divergent angiocrine signals from vascular niche balance liver regeneration and fibrosis. *Nature* **2014**, *505*, 97–102. [CrossRef] [PubMed]
- 5. Song, Y.N.; Zhang, G.B.; Lu, Y.Y.; Chen, Q.L.; Yang, L.; Wang, Z.T.; Liu, P.; Su, S.B. Huangqi decoction alleviates dimethylnitrosamine-induced liver fibrosis: An analysis of bile acids metabolic mechanism. *J. Ethnopharmacol.* **2016**, 189, 148–156. [CrossRef] [PubMed]
- 6. Kirs, S.; Kliewers, A.; Mangelsdorfd, J. Roles of FGF19 in liver metabolism. Cold Spring Harb. Symp. Quant. Biol. 2011, 76, 139–144.
- 7. Zollner, G.; Marschall, H.U.; Wagner, M.; Trauner, M. Role of nuclear receptors in the adaptive response to bile acids and cholestasis: Pathogenetic and therapeutic considerations. *Mol. Pharm.* **2006**, *3*, 231–251. [CrossRef]
- 8. Hu, C.; Zhao, L.; Li, L. Current understanding of adipose-derived mesenchymal stem cell-based therapies in liver diseases. *Stem Cell Res. Ther.* **2019**, *10*, 199. [CrossRef]
- 9. Yuan, Y.; Ni, S.; Zhuge, A.; Li, L.; Li, B. Adipose-Derived Mesenchymal Stem Cells Reprogram M1 Macrophage Metabolism via PHD2/HIF-1α Pathway in Colitis Mice. *Front. Immunol.* **2022**, *13*, 859806. [CrossRef]
- 10. Zhai, L.; Shen, H.; Sheng, Y.; Guan, Q. ADMSC Exo-MicroRNA-22 improve neurological function and neuroinflammation in mice with Alzheimer's disease. *J. Cell. Mol. Med.* **2021**, 25, 7513–7523. [CrossRef]
- 11. Freitag, J.; Bates, D.; Wickham, J.; Shah, K.; Huguenin, L.; Tenen, A.; Paterson, K.; Boyd, R. Adipose-derived mesenchymal stem cell therapy in the treatment of knee osteoarthritis: A randomized controlled trial. *Regen. Med.* 2019, 14, 213–230. [CrossRef] [PubMed]
- 12. Natali, S.; Screpis, D.; Patania, E.; De Berardinis, L.; Benoni, A.; Piovan, G.; Iacono, V.; Magnan, B.; Gigante, A.P.; Zorzi, C. Efficacy and Long-Term Outcomes of Intra-Articular Autologous Micro-Fragmented Adipose Tissue in Individuals with Glenohumeral Osteoarthritis: A 36-Month Follow-Up Study. *J. Pers. Med.* 2023, 13, 1309. [CrossRef] [PubMed]
- 13. Zhang, J.; Zhou, S.; Zhou, Y.; Feng, F.; Wang, Q.; Zhu, X.; Ai, H.; Huang, X.; Zhang, X. Hepatocyte growgrthfactor gene-modified adipose-derived mesenchymal stem cells ameliorate radiation induced liver damage in a rat model. *PLoS ONE* **2014**, *9*, e114670.
- 14. Almalkis, G.; Agrawald, K. Key transcription factors in the differentiation of mesenchymal stem cells. *Differentiation* **2016**, 92, 41–51. [CrossRef] [PubMed]
- 15. Ge, Y.; Zhang, Q.; Li, H.; Bai, G.; Jiao, Z.; Wang, H. Adipose-derived stem cells alleviate liver apoptosis induced by ischemia-reperfusion and laparoscopic hepatectomy in swine. *Sci. Rep.* **2018**, *8*, 16878. [CrossRef]
- 16. Ge, Y.; Zhang, Q.; Jiao, Z.; Li, H.; Bai, G.; Wang, H. Adipose-derived stem cells reduce liver oxidative stress and autophagy induced by ischemia-reperfusion and hepatectomy injury in swine. *Life Sci.* **2018**, 214, 62–69. [CrossRef]

17. Harn, H.J.; Lin, S.Z.; Hung, S.H.; Subeq, Y.M.; Li, Y.S.; Syu, W.S.; Ding, D.C.; Lee, R.P.; Hsieh, D.K.; Lin, P.C.; et al. Adipose-derived stem cells can abrogate chemical-induced liver fibrosis and facilitate recovery of liver function. *Cell Transplant*. **2012**, 21, 2753–2764. [CrossRef]

- 18. Okura, H.; Soeda, M.; Morita, M.; Fujita, M.; Naba, K.; Ito, C.; Ichinose, A.; Matsuyama, A. Therapeutic potential of human adipose tissue-derived multi-lineage progenitor cells in liver fibrosis. *Biochem. Biophys. Res. Commun.* **2015**, 456, 860–865. [CrossRef]
- 19. Yu, F.; Ji, S.; Su, L.; Wan, L.; Zhang, S.; Dai, C.; Wang, Y.; Fu, J.; Zhang, Q. Adipose-derived mesenchymal stem cells inhibit activation of hepatic stellate cells in vitro and ameliorate rat liver fibrosis in vivo. *J. Formos. Med. Assoc. Taiwan Yi Zhi* 2015, 114, 130–138. [CrossRef]
- 20. Huang, K.C.; Chuang, M.H.; Lin, Z.S.; Lin, Y.-C.; Chen, C.-H.; Chang, C.-L.; Huang, P.-C.; Syu, W.-S.; Chiou, T.-W.; Hong, Z.-H.; et al. Transplantation with GXHPC1 for Liver Cirrhosis: Phase 1 Trial. *Cell Transplant*. **2019**, 28 (Suppl. 1), 100s–111s. [CrossRef]
- 21. Pannala, V.R.; Vinnakota, K.C.; Rawls, K.D.; Estes, S.K.; O'Brien, T.P.; Printz, R.L.; Papin, J.A.; Reifman, J.; Shiota, M.; Young, J.D.; et al. Mechanistic identification of biofluid metabolite changes as markers of acetaminophen-induced liver toxicity in rats. *Toxicol. Appl. Pharmacol.* **2019**, 372, 19–32. [CrossRef] [PubMed]
- 22. Zhu, H.; Wang, Z.; Wu, Y.; Jiang, H.; Zhou, F.; Xie, X.; Wang, R.; Hua, C. Untargeted metabonomics reveals intervention effects of chicory polysaccharide in a rat model of non-alcoholic fatty liver disease. *Int. J. Biol. Macromol.* **2019**, *128*, 363–375. [CrossRef] [PubMed]
- Gao, X.X.; Shi, D.H.; Chen, Y.X.; Cui, J.T.; Wang, Y.R.; Jiang, C.P.; Wu, J.H. The therapeutic effects of tectorigenin on chemically induced liver fibrosis in rats and an associated metabonomic investigation. *Arch. Pharmacal Res.* 2012, 35, 1479–1493. [CrossRef] [PubMed]
- 24. Guo, J.; Mo, J.; Zhao, Q.; Han, Q.; Kanerva, M.; Iwata, H.; Li, Q. De novo transcriptomic analysis predicts the effects of phenolic compounds in Ba River on the liver of female sharpbelly (*Hemiculter lucidus*). *Environ. Pollut.* **2020**, 264, 114642. [CrossRef] [PubMed]
- 25. Wu, S.; Ji, X.; Wang, J.; Wu, H.; Han, J.; Zhang, H.; Xu, J.; Qian, M. Fungicide bromuconazole has the potential to induce hepatotoxicity at the physiological, metabolomic and transcriptomic levels in rats. *Environ. Pollut.* **2021**, 280, 116940. [CrossRef]
- Chen, S.; Huang, Y.; Su, H.; Zhu, W.; Wei, Y.; Long, Y.; Shi, Y.; Wei, J. The Integrated Analysis of Transcriptomics and Metabolomics Unveils the Therapeutical Effect of Asiatic Acid on Alcoholic Hepatitis in Rats. *Inflammation* 2022, 45, 1780–1799. [CrossRef]
- 27. Dong, S.; Chen, Q.L.; Song, Y.N.; Sun, Y.; Wei, B.; Li, X.Y.; Hu, Y.Y.; Liu, P.; Su, S.B. Mechanisms of CCl4-induced liver fibrosis with combined transcriptomic and proteomic analysis. *J. Toxicol. Sci.* **2016**, *41*, 561–572. [CrossRef]
- 28. Weber, L.W.; Boll, M.; Stampfl, A. Hepatotoxicity and mechanism of action of haloalkanes: Carbon tetrachloride as a toxicological model. *Crit. Rev. Toxicol.* **2003**, *33*, 105–136. [CrossRef]
- 29. Zhou, J.; Huang, N.; Guo, Y.; Cui, S.; Ge, C.; He, Q.; Pan, X.; Wang, G.; Wang, H.; Hao, H. Combined obeticholic acid and apoptosis inhibitor treatment alleviates liver fibrosis. *Acta Pharm. Sin. B* **2019**, *9*, 526–536. [CrossRef]
- 30. Wang, Y.; Lian, F.; Li, J.; Fan, W.; Xu, H.; Yang, X.; Liang, L.; Chen, W.; Yang, J. Adipose derived mesenchymal stem cells transplantation via portal vein improves microcirculation and ameliorates liver fibrosis induced by CCl4 in rats. *J. Transl. Med.* **2012**, *10*, 133. [CrossRef]
- 31. Chen, L.; Zhang, N.; Huang, Y.; Zhang, Q.; Fang, Y.; Fu, J.; Yuan, Y.; Chen, L.; Chen, X.; Xu, Z.; et al. Multiple Dimensions of using Mesenchymal Stem Cells for Treating Liver Diseases: From Bench to Beside. *Stem Cell Rev. Rep.* 2023, 19, 2192–2224. [CrossRef] [PubMed]
- 32. Begley, M.; Gahan, C.G.; Hill, C. The interaction between bacteria and bile. FEMS Microbiol. Rev. 2005, 29, 625–651. [CrossRef] [PubMed]
- 33. La Frano, M.R.; Hernandez-Carretero, A.; Weber, N.; Borkowski, K.; Pedersen, T.L.; Osborn, O.; Newman, J.W. Diet-induced obesity and weight loss alter bile acid concentrations and bile acid-sensitive gene expression in insulin target tissues of C57BL/6J mice. *Nutr. Res.* **2017**, *46*, 11–21. [CrossRef] [PubMed]
- 34. Lim, K.; Crawfordj, M. The pathology of cholestasis. Semin. Liver Dis. 2004, 24, 21–42.
- 35. Jiao, N.A.; Baker, S.S.; Chapa-Rodriguez, A.; Liu, W.; Nugent, C.A.; Tsompana, M.; Mastrandrea, L.; Buck, M.J.; Baker, R.D.; Genco, R.J.; et al. Suppressed hepatic bile acid signalling despite elevated production of primary secondary bile acids in, NAFLD. *Gut* 2018, 67, 1881–1891. [CrossRef] [PubMed]
- 36. Li, N.; Wang, B.; Wu, Y.; Luo, X.; Chen, Z.; Sang, C.; Xiong, T. Modification effects of SanWei GanJiang Powder on liver and intestinal damage through reversing bile acid homeostasis. *Biomed. Pharmacother.* **2019**, *116*, 109044. [CrossRef]
- 37. Wu, J.S.; Li, Y.F.; Li, Y.Y.; Dai, Y.; Li, W.K.; Zheng, M.; Shi, Z.C.; Shi, R.; Wang, T.M.; Ma, B.L.; et al. Huangqi Decoction Alleviates Alpha-Naphthylisothiocyanate Induced Intrahepatic Cholestasis by Reversing Disordered Bile Acid and Glutathione Homeostasis in Mice. *Front. Pharmacol.* **2017**, *8*, 938. [CrossRef]
- 38. Xie, G.; Jiang, R.; Wang, X.; Liu, P.; Zhao, A.; Wu, Y.; Huang, F.; Liu, Z.; Rajani, C.; Zheng, X.; et al. Conjugated secondary 12α-hydroxylated bile acids promote liver fibrogenesis. *EBioMedicine* **2021**, *66*, 103290. [CrossRef]
- 39. Schneider, K.M.; Candels, L.S.; Hov, J.R.; Myllys, M.; Hassan, R.; Schneider, C.V.; Wahlström, A.; Mohs, A.; Zühlke, S.; Liao, L.; et al. Gut microbiota depletion exacerbates cholestatic liver injury via loss of FXR signalling. *Nat. Metab.* **2021**, *3*, 1228–1241. [CrossRef]

40. Cai, F.F.; Wu, R.; Song, Y.N.; Xiong, A.Z.; Chen, X.L.; Yang, M.D.; Yang, L.; Hu, Y.; Sun, M.Y.; Sun, S.B. Yinchenhao Decoction Alleviates Liver Fibrosis by Regulating Bile Acid Metabolism and TGF-β/Smad/ERK Signalling Pathway. *Sci. Rep.* **2018**, *8*, 15367. [CrossRef]

- 41. Paridaens, A.; Raevens, S.; Colle, I.; Bogaerts, E.; Vandewynckel, Y.; Verhelst, X.; Hoorens, A.; van Grunsven, L.A.; Van Vlierberghe, H.; Geerts, A.; et al. Combination of tauroursodeoxycholic acid and N-acetylcysteine exceeds standard treatment for acetaminophen intoxication. *Liver Int.* 2017, 37, 748–756. [CrossRef] [PubMed]
- 42. Shi, C.; Yang, J.; Hu, L.; Liao, B.; Qiao, L.; Shen, W.; Xie, F.; Zhu, G. Glycochenodeoxycholic acid induces stemness and chemoresistance via the STAT3 signaling pathway in hepatocellular carcinoma cells. *Aging* **2020**, *12*, 15546–15555. [CrossRef] [PubMed]
- 43. Chiangj, Y.L.; Ferrellj, M. Up to date on cholesterol 7 alpha-hydroxylase (CYP7A1) in bile acid synthesis. *Liver Res.* **2020**, *4*, 47–63. [CrossRef] [PubMed]
- 44. He, H.; Mennone, A.; Boyer, J.L.; Cai, S.-Y. Combination of retinoic acid and ursodeoxycholic acid attenuates liver injury in bile duct-ligated rats and human hepatic cells. *Hepatology* **2011**, *53*, 548–557. [CrossRef] [PubMed]
- 45. Fader, K.A.; Nault, R.; Zhang, C.; Kumagai, K.; Harkema, J.R.; Zacharewski, T.R. 2,3,7,8-Tetrachlorodibenzo-p-dioxin (TCDD)-elicited effects on bile acid homeostasis: Alterations in biosynthesis, enterohepatic circulation, and microbial metabolism. *Sci. Rep.* **2017**, *7*, 5921. [CrossRef] [PubMed]
- 46. Doege, H.; Baillie, R.A.; Ortegon, A.M.; Tsang, B.; Wu, Q.; Punreddy, S.; Hirsch, D.; Watson, N.; Gimeno, R.E.; Stahl, A. Targeted deletion of FATP5 reveals multiple functions in liver metabolism: Alterations in hepatic lipid homeostasis. *Gastroenterology* **2006**, 130, 1245–1258. [CrossRef] [PubMed]
- 47. Anderson, C.M.; Stahl, A. SLC27 fatty acid transport proteins. Mol. Asp. Med. 2013, 34, 516–528. [CrossRef] [PubMed]
- 48. Jia, H.M.; Yu, M.; Ma, L.Y.; Zhang, H.W.; Zou, Z.M. Chaihu-Shu-Gan-San regulates phospholipids and bile acid metabolism against hepatic injury induced by chronic unpredictable stress in rat. *J. Chromatogr. B* **2017**, *1064*, 14–21. [CrossRef]
- 49. Claytonp, P.T. Disorders of bile acid synthesis. J. Inherit. Metab. Dis. 2011, 34, 593-604. [CrossRef]
- 50. Yu, X.H.; Qian, K.; Jiang, N.; Zheng, X.L.; Cayabyab, F.S.; Tang, C.K. ABCG5/ABCG8 in cholesterol excretion and atherosclerosis. *Clin. Chim. Acta Int. J. Clin. Chem.* **2014**, 428, 82–88. [CrossRef]
- 51. Hassan, A.S.; Bunick, D.; Lund, L.A.; Bottje, W.G. Glutathione and bile acid synthesis. Effect of GSH content of HepG2 cells on the activity and mRNA levels of cholesterol 7 alpha-hydroxylase. *Biochem. Pharmacol.* 1992, 44, 1475–1477. [CrossRef] [PubMed]
- 52. Cunningham, T.J.; Duester, G. Mechanisms of retinoic acid signalling and its roles in organ and limb development. *Nat. Rev. Mol. Cell Biol.* **2015**, *16*, 110–123. [CrossRef] [PubMed]
- 53. Bono, M.R.; Tejon, G.; Flores-Santibañez, F.; Fernandez, D.; Rosemblatt, M.; Sauma, D. Retinoic Acid as a Modulator of T Cell Immunity. *Nutrients* **2016**, *8*, 349. [CrossRef] [PubMed]
- 54. Podolak-Popinigis, J.; Górnikiewicz, B.; Ronowicz, A.; Sachadyn, P. Transcriptome profiling reveals distinctive traits of retinol metabolism and neonatal parallels in the MRL/MpJ mouse. *BMC Genom.* **2015**, *16*, 926. [CrossRef]
- 55. Jiang, Y.; Li, C.; Chen, L.; Wang, F.; Zhou, X. Potential role of retinoids in ovarian physiology and pathogenesis of polycystic ovary syndrome. *Clin. Chim. Acta* **2017**, *469*, 87–93. [CrossRef]
- 56. Baybutt, R.C.; Hu, L.; Molteni, A. Vitamin A deficiency injures lung and liver parenchyma and impairs function of rat type II pneumocytes. *J. Nutr.* **2000**, *130*, 1159–1165.
- 57. Chen, H.; Kan, Q.; Zhao, L.; Ye, G.; He, X.; Tang, H.; Shi, F.; Zou, Y.; Liang, X.; Song, X.; et al. Prophylactic effect of Tongxieyaofang polysaccharide on depressive behavior in adolescent male mice with chronic unpredictable stress through the microbiome-gutbrain axis. *Biomed. Pharmacother.* **2023**, *161*, 114525. [CrossRef]

Disclaimer/Publisher's Note: The statements, opinions and data contained in all publications are solely those of the individual author(s) and contributor(s) and not of MDPI and/or the editor(s). MDPI and/or the editor(s) disclaim responsibility for any injury to people or property resulting from any ideas, methods, instructions or products referred to in the content.